An accurate and efficient decoupling approximation for temperature-dependent multimode resonance Raman spectra

John M. Jean and Richard A. Friesner
Department of Chemistry, The University of Texas at Austin, Austin, Texas 78712

(Received 18 September 1985; accepted 15 May 1986)

We present two advances in the use of the matrix method to generate the time-dependent kernel for resonance Raman scattering. The first of these, a collocation method, allows a substantial decrease in computation time in addition to greater resolution of scattered profiles. Second, we have developed a decoupling approximation in which the exact method of Friesner *et al.* is used to generate the kernel at a relatively small number of time points with the remaining points obtained by fitting to the exact values a factorized expression containing both finite temperature and dephasing corrections. The approximation is exact in the zero temperature limit and is based on a sum rule which ensures exact reproduction of integrated intensities. Calculations with a wide variety of parameter values are presented and show that our approximate method is highly accurate in reproducing the exact results for a wide variety of physically realistic systems. In addition, our results for single mode systems are shown to compare favorably to those obtained using a transform-based method.

I. INTRODUCTION

In a recent paper,[1] we presented a method for constructing the exact time domain kernel for resonance Raman scattering of a molecule described by harmonic ground and excited state potential surfaces. This approach allows accurate simulation of temperature dependent excitation *and* scattering profiles for large-dimensional multimode systems even if Duschinsky rotation is important, and hence represents an advance in capabilities over previous time domain[2,5–9] and sum-over-states methods.

However, the above formulation necessitates a three-dimensional Fourier transform to generate spectral line shapes, thus greatly increasing computation times. While this price will be worth paying on occasion, the reported values would lead to undesirable expenditures when, e.g., extensive parameter fitting to experiments is required. These considerations have motivated us to develop a new approximate technique, and to test an existing efficient method (the transform method introduced by Hizhnyakov and co-workers[4] and further developed by Page and co-workers[5–9]) against exact results. We have also made several technical improvements in our numerical methods which generally reduce computation times for both the old and new methods.

Our approximation scheme (a decoupling procedure with explicit correlation corrections) is one to two orders of magnitude faster than the full three-dimensional transform, and achieves acceptable accuracy (within typical experimental resonance Raman noise levels) for the great majority of parameter values we have tested. It is exact in the low-temperature limit, and satisfies a sum rule such that the integrated intensity of any excitation profile is guaranteed to be exact (so that reliable absolute intensities can be calculated). Computation times are roughly five to ten times larger than for a transform based method which employs a microscopic model[7]; the latter approach, however, will be shown to break down at high temperatures and/or large values of linear or quadratic coupling (as is discussed in Ref. 9). The transform method *is* adequate as long as parameter values are sufficiently far from these limits (and absolute intensities are not desired), and thus remains as an attractive approach to a wide variety of practical problems.

The paper is organized into six sections. In Sec. II we formally develop the decoupling approximation and introduce a collocation method[12] which greatly improves resolution in scattering profiles and reduces computation times. In Sec. III, extensive comparison of excitation profiles obtained by the three methods (exact, decoupling, and transform) for a range of single mode models (varying temperature, linear coupling, and quadratic coupling) are presented. In Sec. IV, we investigate decoupled and exact results for Duschinsky coupled multimode systems (the transform method is not directly applicable to such cases although a related approach which is applicable has recently been developed[13]). Section V presents some results of the decoupling theory for multimode scattering profiles; these correspond to what is actually measured in an overwhelming majority of resonance Raman experiments. In Sec. VI, the conclusion, future developments are suggested, and an assessment of the various time domain methods discussed here is undertaken.

II. THEORY

A. Collocation method

The exact Raman kernel K is dependent on the three time variables t, t', and μ; we can express this in the form

$$K(t,t',\mu) = \sum_{n=1}^{N} F_n(t,t')\exp(i\omega_n\mu) . \quad (1)$$

Here the set $\{\omega_n\}_{n=1}^{N}$ comprise the set of *observable* Raman scattering peaks [otherwise, $F_n(t,t') \sim 0$] and hence are in principle obtainable from experiment. For the moment, we fix t and t' so that the $F_n(t,t')$ can be thought of as static coefficients; then, the F_n can be efficiently determined by a collocation[12] (or interpolation) technique. Evaluating $K(t,t',\mu)$ at the points $\mu_1 \ldots \mu_N$, we solve the matrix equations $\mathbf{RF} = \mathbf{K}$ for $\mathbf{F}$, i.e., $\mathbf{F} = \mathbf{R}^{-1}\mathbf{K}$ where

 0021-9606/86/172353-12$02.10

$\mathbf{F} = [F_1(t,t'),...,F_N(t,t')]$, $\mathbf{K} = [K(t,t',\mu_1),...,K(t,t',\mu_N)]$, and $\mathbf{R}$ is the function matrix $R_{ij} = \exp(i\mu_i\omega_j)$. If the set $\{\omega_n\}$ is nearly complete for the kernel $K(t,t',\mu)$ (a condition readily achieved in practice, as will be shown below), the error in this procedure is quite small.

For a single mode, the ω_j are equally spaced (representing overtones and anti-Stokes lines), and upon choice of the appropriate equally spaced μ_i, the method is equivalent to a discrete Fourier transform. For unequally spaced frequencies, a nonlinear least-squares routine is used to optimize the collocation points. The latter technique will not be explicitly employed in this paper, but it is an integral aspect of practical multimode simulations, and will be discussed at length in a future publication.

Application of the above procedure for each t and t' yields a set of kernels $F_n(t,t')$. For delta-function scattering peaks, the excitation profile of the frequency ω_n is then

$$I_n(E) = \int_0^\infty \int_0^\infty dt\,dt' \exp[-iE(t'-t)] \times \exp[-\Gamma(t+t')]F_n(t,t') , \quad (2)$$

where Γ is an electronic relaxation parameter.

If we assign each scattering peak a line shape function $L_n(\omega_n,\omega)$, a complete scattering profile at laser excitation energy E is obtained via

$$I_E(\omega) = \sum_n I_n(E) L_n(\omega_n,\omega) .$$

Thus, determination of the $F_n(t,t')$ completely specifies the entire set of Raman data.

Application of the above procedure to the exact three-dimensional approach of Ref. 1 allows considerable reduction of the number of μ time points and enhanced resolution of scattering peaks for systems with a moderate number of high frequency modes. When a large number of low frequency modes are to be explicitly included in the calculation, basis functions of the form $\exp(i\omega_n\mu)$ become ineffective; instead, other functional forms (e.g., Lorentzian or Gaussian functions) should be used in Eq. (1). This will be investigated in subsequent work.

B. Decoupling approximation

Our basic approach throughout this section will be to calculate the exact $F_n(t,t')$ using the matrix method of Ref. 1 (see also Refs. 10 and 11) at a limited number of points (t,t'), and fit our approximate function to these points. The fundamental structure guarantees exact results in the low temperature limit. On this base is superimposed satisfaction of a sum rule ensuring exact integrated excitation profiles, and a correlation function which depends explicitly on $t-t'$ to dephase the correction term at large $t-t'$ separations. This last modification is required if the sum rule imposition is to be maintained for high temperatures.

It is easily shown (see the Appendix) that, at low temperature, the functions $F_n(t,t')$ factor (or decouple) into a form

$$F_n(t,t') = A_n(t)\,A_n^+(t') . \quad (3)$$

This expression is also approximately valid at small t and t', as shown in the Appendix.

The function $A_n(t)$ is obtained as follows. We choose a small value of t (t_0) such that $\omega_n t_0 \ll 1$ and calculate $F_n(t_0,-t_0)$; then from Eq. (3),

$$A_n(t_0) = [F_n(t_0,-t_0)]^{1/2} . \quad (4)$$

The set $F_n(t_1,t_0),...,F_n(t_N,t_0)$ are then obtained [$t_1,...,t_N$ are equally spaced time points, to be Fourier transformed over as in Eq. (2)] to yield

$$A_n(t_j) = F_n(t_j,t_0)/A_n^+(t_0) . \quad (5)$$

At low temperatures, this procedure alone is sufficient to yield highly accurate results. Numerous calculations using different values for t_0 show that the approximate kernel is insensitive to this parameter as long as $\omega_n t_0 \ll 1$. This is illustrated numerically in Table V in the Appendix which compares the approximate values of $F(t,t')$ obtained using three different values of t_0 with those obtained from the exact method.

A useful improvement at finite temperature can be obtained by noting that the zeroth moment (integrated intensity) of an excitation profile is given by

$$\begin{aligned} M_0 &= \int_{-\infty}^{\infty} I_n(E)dE \\ &= \iiint dE \exp[i(t-t')E]e^{-\Gamma(t+t')}F_n(t,t')dt\,dt' \\ &= \iint \delta(t-t')\exp[-\Gamma(t+t')]F_n(t,t')dt\,dt' \\ &= \int dt\,F_n(t,t)\exp(-2\Gamma t) . \end{aligned}$$

Thus M_0 depends *only* on $F_n(t,t)$; by fitting our approximate function to the exact F_n at all pairs (t_j,t_j), we ensure that the correct M_0 is obtained. To do this, we take as an ansatz a new functional form

$$F_n(t,t') = [1+G(t)G(t')]A_n(t)A_n^+(t') . \quad (6)$$

Because the exact $F_n(t,t)$ is real, $G(t)$ is also real. At small t, $G(t)\to 0$, so our procedure in finding $A_n(t)$ [Eqs. (4) and (5)] is still valid because $G(t_0)$ can be approximated as zero. $G(t)$ is then found via

$$G(t) = \left[\frac{F_n(t,t)}{|A_n(t)|^2} - 1\right]^{1/2} .$$

We have always found that the quantity in brackets on the right-hand side is greater than zero.

A problem arises for high temperature and large quadratic coupling or mode mixing. For these cases, $G(t)$ becomes quite large; then the assumption $G(t_0)\cdot G(t) \approx 0$ is no longer rigorously valid, and serious errors in $F_n(t,t')$ for large $|t-t'|$ result. This difficulty is remedied by introduction of an explicit dephasing function $H(t-t')$. We choose a value t_1 such that $G(t_1)\approx 1$ and compute the exact $F_n(t_1,t')$ for all t'. The accuracy of the calculations are not sensitive to the precise value of t_1 chosen.

We take as our final ansatz

$$F_n(t,t') = [1+G(t)G(t')H(t-t')]A_n(t)\,A_n^+(t') . \quad (7)$$

[Note that $H(t-t')$ must equal $H^+(t'-t)$ in order for our

approximation to preserve the exact symmetry $F_n(t,t') = F_n^+(t',t)$.]

We obtain H via

$$H(t_1 - t') = \left[\frac{F_n(t_1,t')}{A_n(t)A_n^+(t')} - 1\right]/G(t)G(t') \quad (8)$$

so that H is invoked only if Eq. (6) becomes inadequate. Physically, the role of $H(t-t')$ is quite transparent; it damps the correction factor $G(t)G(t')$ when the kernel contains extensive destructive interference (quadratic coupling and mode mixing are particularly effective in creating this). The necessity of this correction can easily be observed by comparing the approximate $F_n(t,t')$ with its exact counterpart directly in the time domain.

The above three-step procedure is easily automated computationally and requires only $3NM$ kernel points (N = number of collocation frequencies, M = number of t points) as opposed to NM^2 points in the method of Ref. 1. Assuming 30–300 time points are required, a factor of 10–100 in reduction of computation time is expected (generation of the kernel is overwhelmingly the most time consuming part of the calculation). This is confirmed explicitly in our numerical results.

C. Fourier transform of the approximate kernel

The excitation profile of a mode ω_n is given by

$$I_n(E) = \int_0^{T_{\max}} \int_0^{T_{\max}} e^{-iE(t'-t)} F_n(t,t') e^{-\Gamma(t+t')} dt\, dt', \quad (9)$$

where $T_{\max}$ is chosen so that $\exp(-\Gamma T_{\max})$ is negligible. To implement this efficiently, we change variables to $t_+ = 1/2(t+t')$, $t_- = 1/2(t-t')$; then

$$I_n(E) = \int_{-T_{\max}}^{T_{\max}} dt_- \exp(iEt_-) \times \int_0^{2t_-} dt_+ e^{-\Gamma t_+} F_n(t_+,t_-) . \quad (10)$$

Symmetry properties of the kernel can then be invoked to yield

$$\mathrm{I_n(E) = 2\,Re}\left[\int_0^{\mathrm{T_{max}}} \mathrm{dt\_\ exp(iEt\_)S(t\_)}\right], \quad (11)$$

where

$$S(t_-) = \int_0^{2t_-} dt_+ e^{-\Gamma t_+} F_n(t_+,t_-).$$

Thus, $S(t_-)$ is only evaluated once, and then employed to compute $I_n(E)$ for all values of E via a one-dimensional Fourier transform (if desired, an FFT can be utilized in the last integration). This reorganization of the integration ensures that these steps require only a small fraction of the total computation time.

D. Block factorization

In a typical practical multimode problem, not all vibrational modes will be coupled via Duschinsky rotation in the excited state. To evaluate the kernel most efficiently, the calculation is divided into a product of coupled blocks, as indicated in Ref. 1. After applying the collocation method to each block, the expression for the overall correlation function for an excitation profile reads

$$F_n(t,t') = \prod_{m=1}^{\mathrm{NB}} f_m^{(n)}(t,t') , \quad (12)$$

where NB is the total number of blocks, and $f_m^{(n)}$ is the appropriate correlation function from each block. The scattering frequency associated with F_n is

$$\omega_n = \sum_m \omega_m^{(n)} .$$

Thus a fundamental of frequency ω_c from block l is composed of one factor $f_l^{(n)}(t,t')$ associated with the collocation function $\exp(i\omega_c\mu)$, while the remaining functions $f_{m\neq l}^{(n)}(t,t')$ are obtained from the $m \neq l$ block Rayleigh lines ($\omega_c = 0$). Similarly, combinations of modes from two different blocks are assembled from the product of $f_{l_1}^{(n)}(t,t') \cdot f_{l_2}^{(n)}(t,t')$ with the remaining Rayleigh functions. In principle, all possible transitions can be obtained by this method; in practice, single and double substitutions should be sufficient in most cases of interest.

In this paper, only results generated from a single block are presented. The block factorization method will, however, yield order of magnitude reductions in computation time for large systems, and is therefore an important adjunct to the present approach. It will be explored in detail in forthcoming work.

III. SINGLE MODE EXCITATION PROFILES

In order to test the validity of our approximation, we have performed numerous calculations on both single and multimode systems using the exact and approximate methods. For one mode systems, we compare our results with those obtained using the transform method of Page and coworkers.[5–9] The transform method results are scaled such that the integrated intensity of an excitation profile is equal to that obtained from the exact matrix method. In our implementation of this approach, we use the excited state frequency in Eq. (3) of Ref. 8, which has been shown to improve accuracy for systems with quadratic coupling. The absorption spectrum required to implement the transform method was computed by using the numerical methods of Ref. 1, with only one exponent combining step being required.

For a single mode, we write the Hamiltonians for the ground and excited states as

$$H^g = \omega/2(b^+b + bb^+) , \quad (13a)$$

$$H^e = H^g + g(b+b^+) + v(b+b^+)^2 , \quad (13b)$$

where ω is the oscillator frequency and b^+, b the boson creation and annihilation operators. The vibronic parameters g and v describe the equilibrium displacement (linear coupling) and frequency shift (quadratic coupling) of the excited state relative to the ground state.

In all the results presented here, we have set the frequency equal to 1.00 and scaled all other parameters to this value. Thus the temperature parameter β is actually $\beta\omega(=\omega/kT)$. Values of $\beta = 1.0$ and 0.5, for example, correspond to room temperature for 200 and 100 cm^{-1} modes, respectively. The linear coupling parameter g is related to the dimen-

TABLE I. Parameters for one mode system ($\omega = 1.00$, $\Gamma = 0.2$).

Case	g	v	β	n_μ
1	0.55	0.00	1.0	12
			0.5	14
2	1.00	0.00	2.0	20
			1.0	22
			0.5	24
3	0.55	−0.10	1.0	16
			0.5	20
4	0.55	0.40	2.0	16
			0.5	24

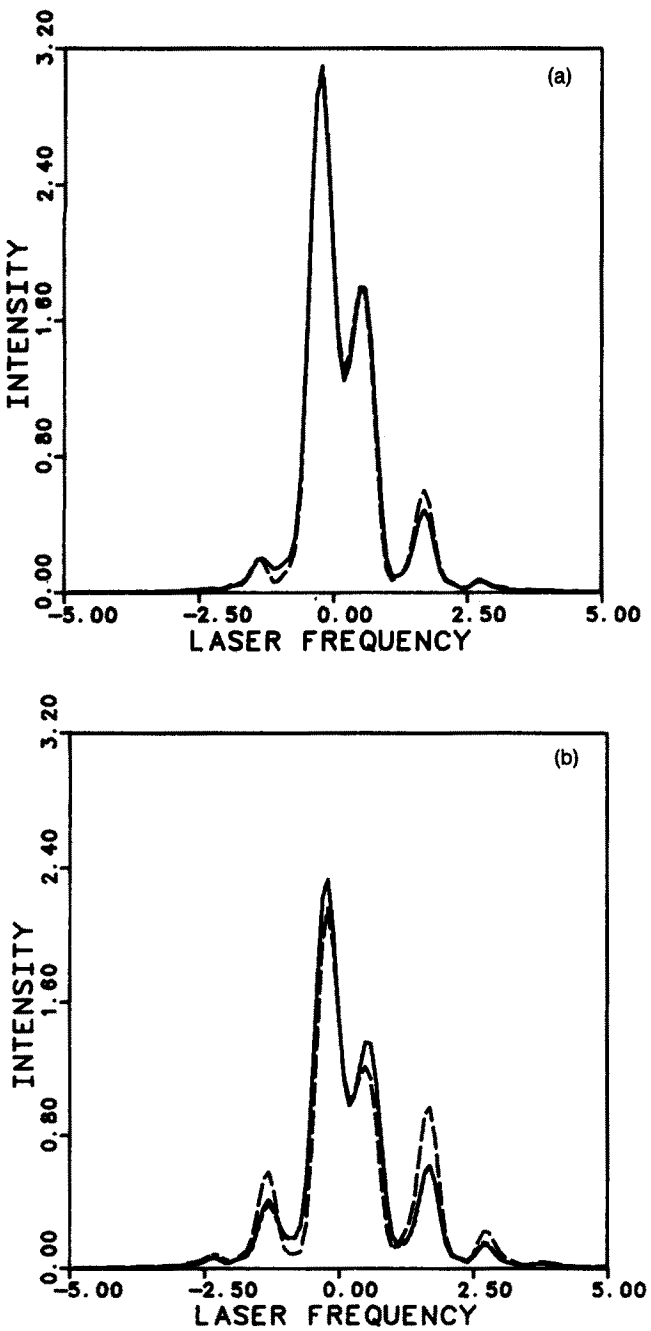

FIG. 1. REP for fundamental of one mode system case 1. (—) exact; (···) decoupled approximation; (---) transform method. (a) $\beta = 1.0$; (b) $\beta = 0.5$.

sionless normal coordinate displacement Δ by the formula

$$g = \frac{-\Delta\omega}{\sqrt{2}}.$$

The quadratic coupling parameter v is related to the excited state frequency by

$$\omega^e = [(\omega^g)^2 + 2v]^{1/2}.$$

The number of time points n_t for the t and t' dimensions in general depends on the resolution desired, and thus will depend on the extent of vibrational dephasing and on the Lorentzian (lifetime) damping factor Γ. Unless otherwise specified, the results discussed in this paper were calculated using $n_t = n_{t'} = 36$ with a damping of $\Gamma = 0.20$.

The number of μ time points, or equivalently the number of collocation frequencies, depends on the number of bands present in the scattered spectrum (anti-Stokes bands included). Large values for the coupling parameters and/or high temperatures naturally require a greater number of points to achieve the desired accuracy. The Hamiltonian parameters along with the number of collocation frequencies for each calculation are shown in Table I. These values were chosen to ensure convergence; one could make do with a smaller number of collocation frequencies with little sacrifice in accuracy.

We begin our discussion of Raman excitation profiles (REP's) for one mode systems by considering an oscillator with moderate displacement in the excited state. The REP of the fundamental is shown in Fig. 1. The quantity plotted as intensity corresponds to $I_n(E)$ in Eq. (2). The abscissa corresponds to the incident frequency minus the zeroth order energy separation of the ground and excited states. Note that the 0–0 band occurs at the Franck–Condon energy shift $\Delta E = -g^2/\omega$.

Since the value of g in this example represents a significant displacement of the excited state, we observe resonances at a number of excited vibronic levels.

For both temperatures chosen, agreement between the exact and approximate matrix method calculations is quantitative (the curves are indistinguishable). While the transform method gives excellent results at $\beta = 1.0$, it breaks down somewhat when the temperature is raised to $\beta = 0.5$. For displaced oscillators with smaller values for g or at lower temperatures, we have found that the decoupled approximation and transform method agree with the exact result.

The breakdown of the transform method at relatively large displacement is further exemplified in Fig. 2, which shows the REP of a one mode system with $g = 1.0$ at three different temperatures. At high temperature we begin to see some discrepancy between the exact and approximate results, although agreement between the two remains quite good.

Since modes with appreciable displacement in the excited state will show significant overtone intensity in the scattered spectrum, an important aspect of any computer simulation of experimental data of such systems will be modeling the overtone REP's in addition to that of the fundamental. As an example, Fig. 3 shows the REP of the first overtone at low and high temperature for the same system shown in Fig. 2.

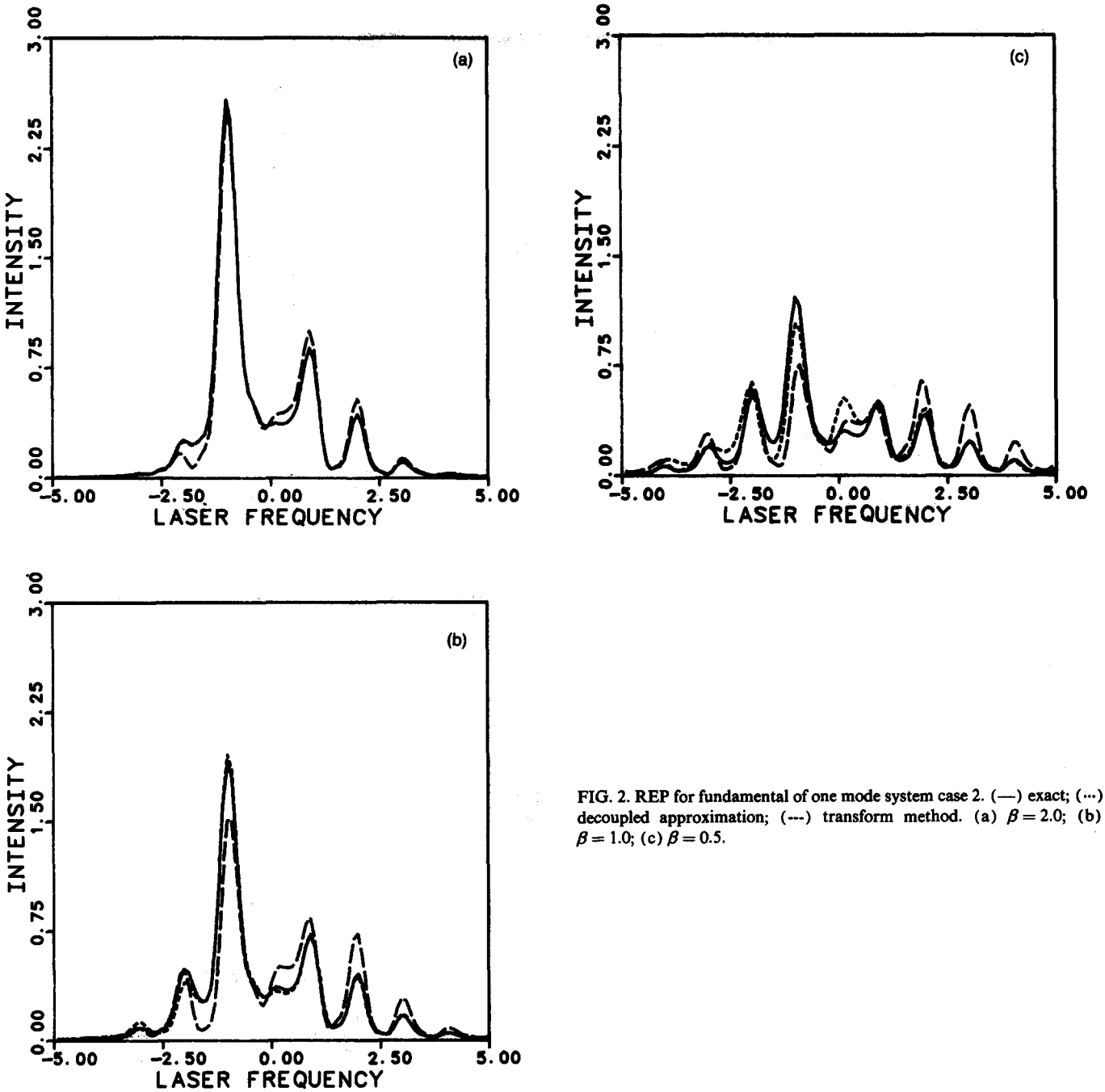

FIG. 2. REP for fundamental of one mode system case 2. (—) exact; (···) decoupled approximation; (---) transform method. (a) $\beta = 2.0$; (b) $\beta = 1.0$; (c) $\beta = 0.5$.

Figures 4 and 5 display REP's for systems which contain both linear and quadratic coupling. It is clear that at high temperatures the transform method consistently overestimates the intensity of the highest energy vibronic peak. While the decoupling approximation displays some discrepancies (especially for high temperature and negative quadratic coupling), it does provide a superior fit in all the cases we have examined.

We have performed a series of calculations with v ranging from ± 0.05 to ± 0.40 (not shown here) with similar results. It is apparent from comparing values of the kernel for the exact and approximate methods directly in the time domain that for systems with negative frequency shifts, representing closer spacing of vibrational levels in the excited state, the form of the correlation function $H(t-t')$ is not valid at all times. Calculation of two functions, one at short times and one at long times, would more closely model the dephasing present in these systems and lead to more accurate results; however, this would necessitate generation of more kernel points using the exact method and lead to increased computation times.

IV. MULTIMODE EXCITATION PROFILES

For systems with more than one mode we generalize Eq. (13) to

$$H^g = \sum_{i=1}^{N} \frac{\omega_i}{2} (b_i^+ b_i + b_i b_i^+) , \tag{14a}$$

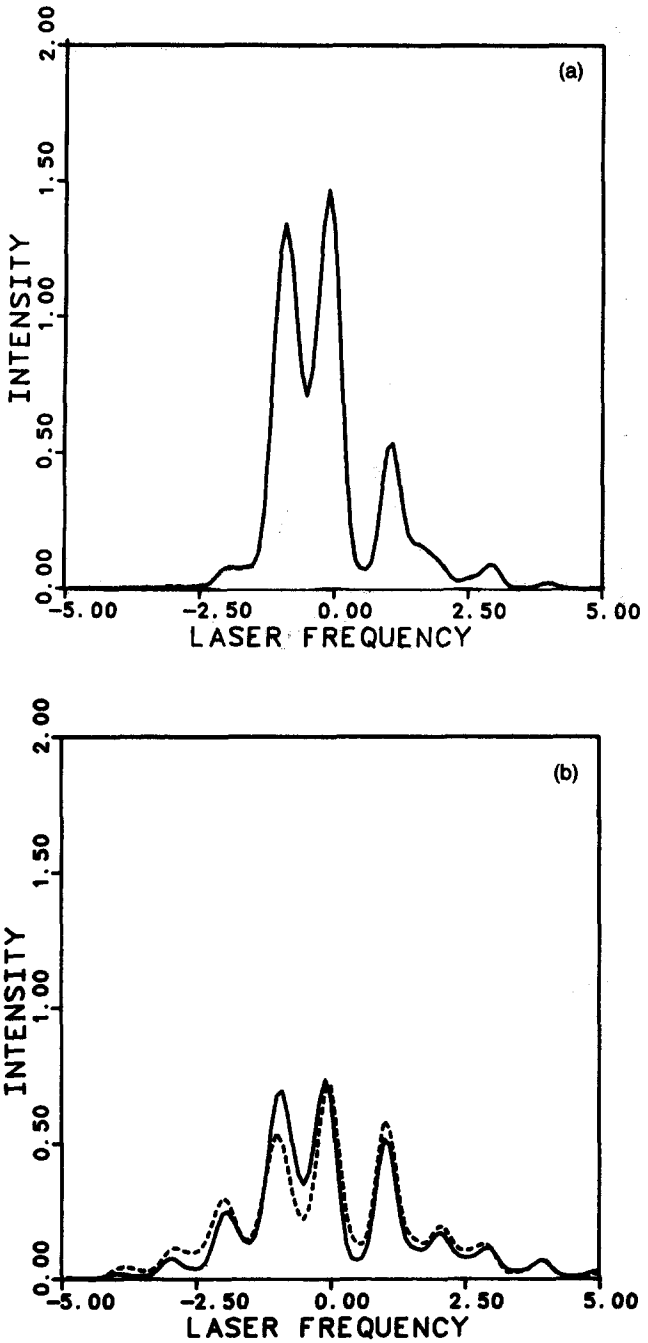

FIG. 3. REP for first overtone of one mode system case 2. (—) exact; (···) decoupled approximation. (a) $\beta = 2.0$; (b) $\beta = 0.5$.

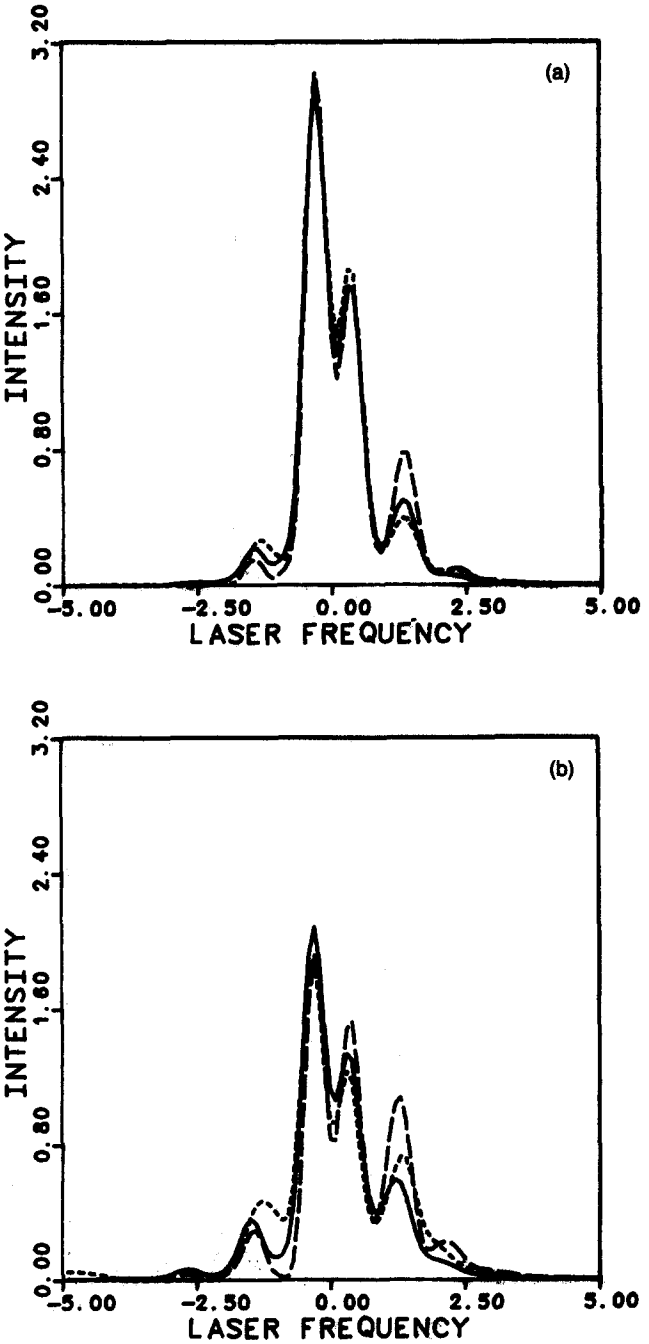

FIG. 4. REP for fundamental of one mode system case 3. (—) exact; (···) decoupled approximation; (---) transform method. (a) $\beta = 1.0$; (b) $\beta = 0.5$.

$$H^e = H^g + \sum_{i=1}^{N} \{g(b_i + b_i^+) + v(b_i + b_i^+)^2\} + \sum_{i=1}^{N} \sum_{j>1} S_{ij}\{(b_i + b_i^+)(b_j + b_j^+) + (b_j + b_j^+)(b_i + b_i^+)\}, \quad (14b)$$

where N is the number of normal modes and S_{ij} elements of the Duschinsky (rotation) matrix. For two mode systems, $2S_{12}(\omega_1\omega_2)^{1/2}$ is the sine of the angle of rotation the normal coordinates experience under electronic excitation.

For multimode systems in which mode mixing does not play a role, the calculation can be factored into a product of one mode calculations with $G(t)$, $A(t)$, and $H(t-t')$ computed for each mode separately. In this section we focus our attention on coupled systems for which such a factorization is impossible.

Figure 6 presents REP's for both modes of a two mode system at $\beta = 1.0$ and 0.5. The Hamiltonian parameters of this system are shown in Table II. In addition to being coupled via Duschinsky rotation, both modes experience significant displacement and frequency shifts in the excited state. Agreement between the exact and approximate methods is

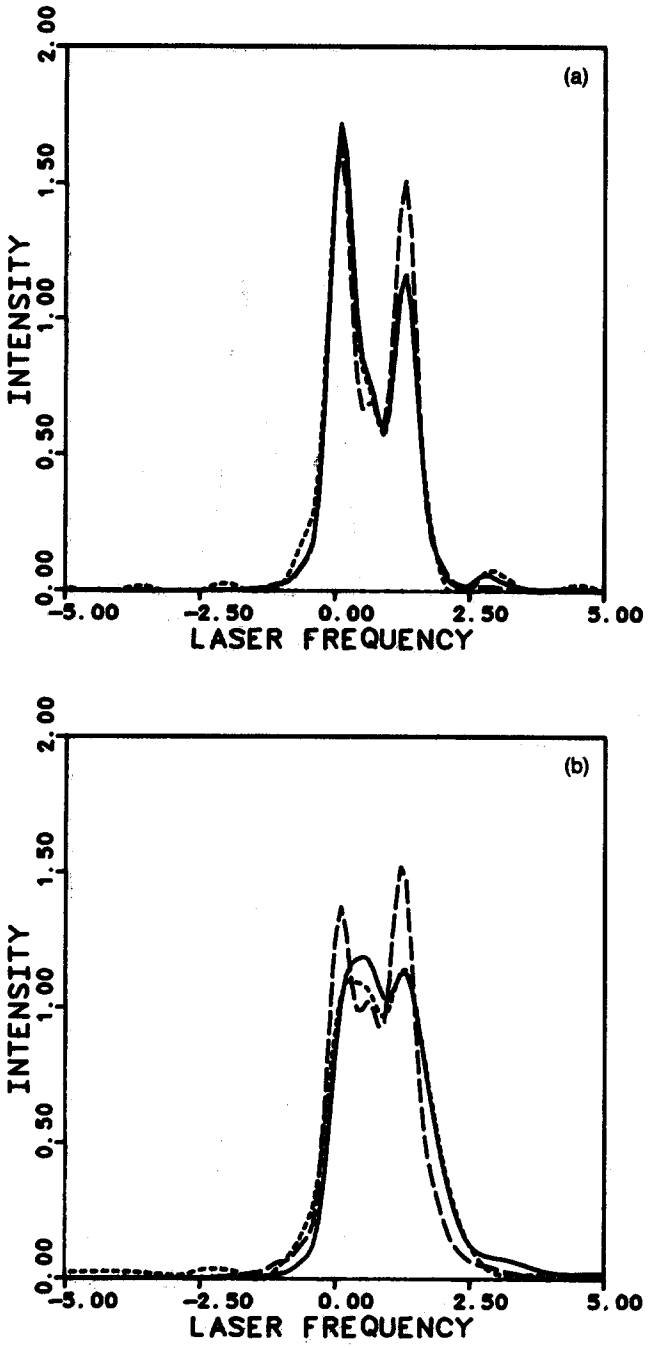

FIG. 5. REP for fundamental of one mode system case 4. (—) exact; (···) decoupled approximation; (---) transform method. (a) $\beta = 2.0$; (b) $\beta = 0.5$.

excellent. In the high temperature spectra, however, we note spurious oscillations in the approximate profile far off resonance. These are manifestations of the problem of modeling the vibrational dephasing in systems which have different ground and excited state frequencies with a single correlation function of the form $H(t-t')$. As can be seen from the spectra, however, these oscillations do not affect accuracy in the region of interest; thus such occurences will present no problems in actual simulations.

Figure 7 shows the REP's for the lowest and highest frequency modes of a coupled five mode system at a temperature of $\beta = 1.0$. The Hamiltonian parameters for this system are shown in Tables III and IV. We define a Duschinsky matrix using the off-diagonal elements in the second order term in the Taylor series expansion of the excited state Hamiltonian.

$$S_{ij} = \left(\frac{\partial^2 H^e}{\partial Q_i \partial Q_j}\right)_{Q_i=0, Q_j=0}.$$

While the decoupling approximation underestimates somewhat the intensity in the resonance region for the lower frequency mode, the overall band shape is quite similar and represents a reasonable approximation to the exact result. For the higher frequency mode, agreement between the approximate and exact profiles is excellent.

V. SCATTERED PROFILES

In Ref. 1 we pointed out a distinct advantage the matrix method has over other time-dependent methods in that the entire Raman surface $I(E,\omega_s)$ is produced.

We have found that in order to achieve a desirable level of resolution for scattering profiles, upwards of 100 time points along the μ time direction must be used if an ordinary Fourier transform in μ is employed. Replacement of the Fourier transform by the collocation method of Sec. II A produces a delta function spectrum which can be used to model a scattered spectrum by assigning each peak a line shape function defined by one or more broadening factors; this procedure generates much more accurate scattering profiles with less computational effort. In the examples presented here, we use a Lorentzian line shape defined by the parameter γ. Extension to other types of functions (Gaussian, Voigt, etc.) presents no difficulties.

Figure 8 shows a scattered spectrum for the one mode example case 2 (Fig. 2). The incident frequency is in resonance with the 0–0 band. The large displacement ($g = 1.0$) coupled with a sparse vibrational manifold produces a long progression.

Scattered profiles for the two mode system of the previous section are presented in Fig. 9. The incident frequencies are approximately in resonance with the 0–0 band (a) and the 0–1 band (b) of the lower frequency mode. For both these cases, the difference between the approximate and exact results is negligible.

Finally, Fig. 10 shows the Raman spectrum of the five mode system with an incident frequency of $\omega_L = 1.0$. For the most part, agreement between the exact and approximate calculations is excellent; however, we note some discrepancies in the overtone region. This example illustrates the limitation of the approximation in treating strongly coupled systems, and points out the need for an exact method if precise quantitative results in all spectral regions are desired.

VI. CONCLUSION

We have presented two significant advances in the use of the matrix method to generate resonance Raman line shapes. The first of these, use of the collocation method, was motivated by the fact that in general we know the entire set of frequencies corresponding to the ground surface before we undertake a computer simulation, so an integral trans-

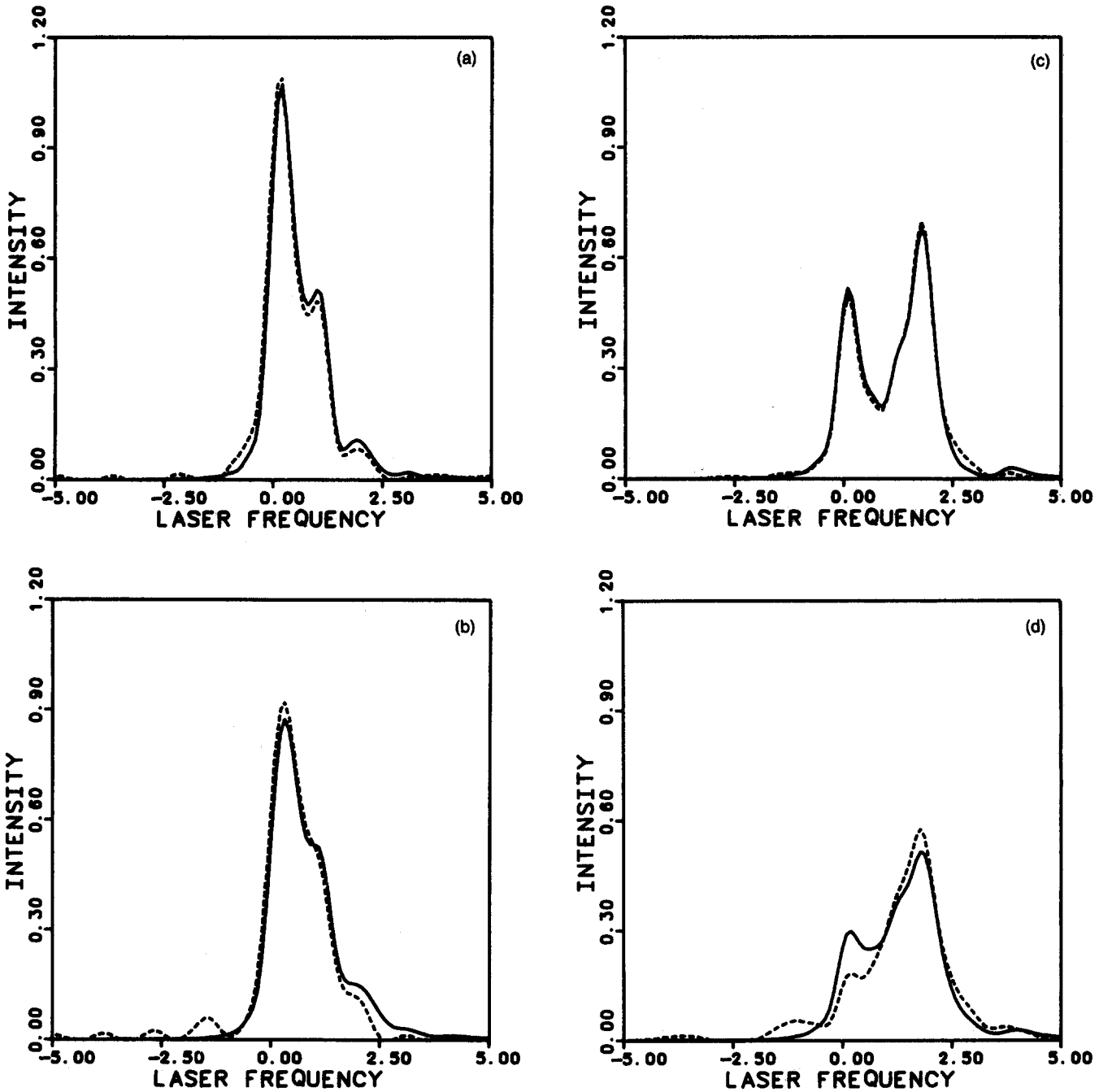

FIG. 6. REP's for the two mode system. (—) exact; (···) decoupled approximation. (a) $\omega_S = 1.00, \beta = 1.00$; (b) $\omega_S = 1.0, \beta = 0.5$; (c) $\omega_S = 1.50, \beta = 1.0$; (d) $\omega_S = 1.50, \beta = 0.5$.

form over a large number of time points and an essentially continuous set of frequencies is inefficient. This advance alone produces a fourfold or more decrease in the computation time.

The second advance is the use of a factorized form for the coefficients $F(t,t')$ appearing in the Fourier expansion for the kernel. This technique necessitates generation of the exact kernel at a relatively small number of time points. Depending on the number of time points required, the decoupled approximation can save from one to two orders of magnitude in time.

We have tested this approximation with a series of one, two, and five mode calculations varying the excited surface over a wide range of geometries. The approximation provides an excellent fit to the exact spectrum in all cases except when there is substantial quadratic coupling at high temperature ($\beta = 0.5$). This value of β corresponds to room

TABLE II. Parameters for two mode systems ($\Gamma = 0.2$).

Mode	w	g	v	β	n_μ
1	1.00	0.40	0.20	1.0	26
2	1.50	0.50	0.30	0.5	30
		$S_{12} = 0.25$			

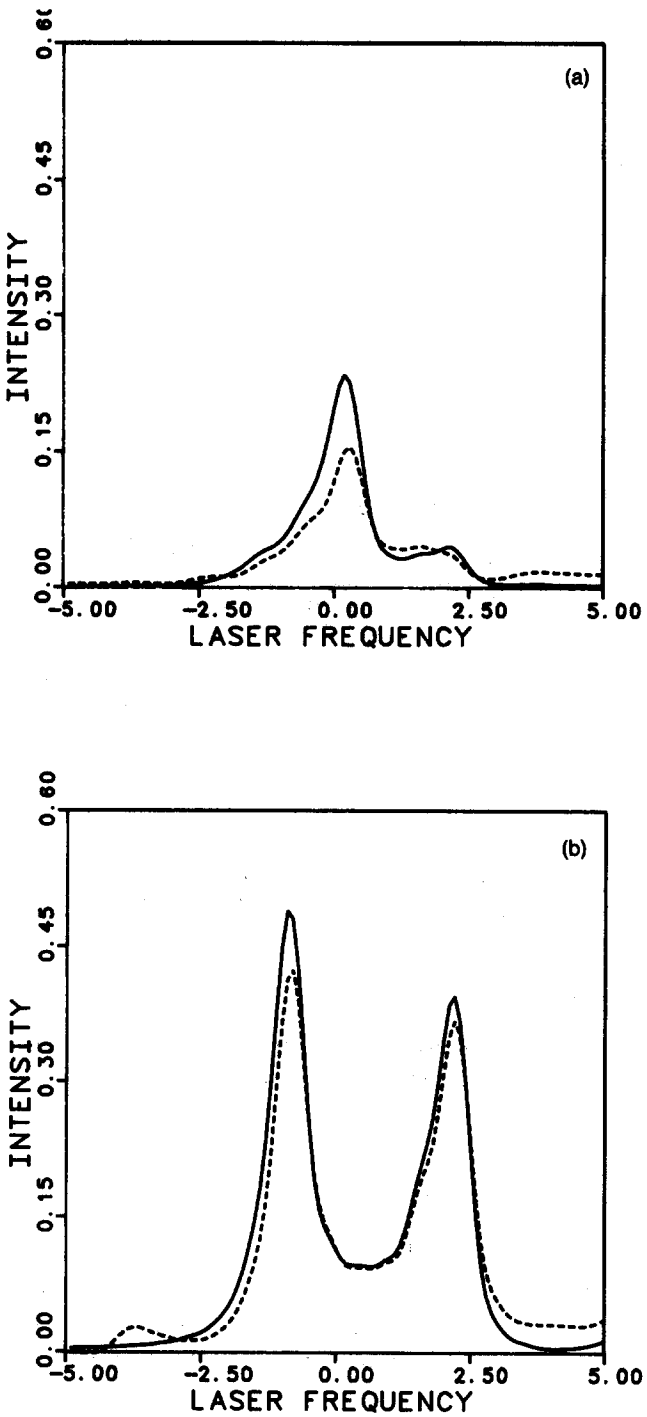

FIG. 7. REP's for the lowest and highest frequency fundamentals for the five mode example. (a) $\omega_S = 1.00$; (b) $\omega_S = 3.00$. B = 1.0.

TABLE III. Parameters for five mode systems ($n_t = n_{t_1} = 36, n_\mu = 40$).

Mode	ω	g	v
1	1.00	0.30	0.30
2	1.25	0.35	−0.20
3	1.75	0.60	−0.25
4	2.25	0.75	0.10
5	3.00	1.20	0.00

TABLE IV. Duschinsky matrix for five mode systems.

Mode	1	2	3	4	5
1	0.00	0.10	0.20	0.20	0.35
2	0.10	0.00	0.10	0.15	0.20
3	0.20	0.10	0.00	0.20	0.25
4	0.20	0.15	0.20	0.00	0.25
5	0.35	0.20	0.25	0.25	0.00

temperature or above only for modes with frequencies of 100 cm^{-1} or less. Highly accurate simulation of such modes would require the exact method; however, the decoupled approximation still provides an excellent starting point for simulation of these types of systems.

For all the one mode cases studied, our approximate method performs as well as or better than the transform method although the latter is more efficient computationally. The method of choice in performing a simulation will depend on the objective of the calculation, the nature of the system, and the desired accuracy.

As discussed in detail in Ref. 9, accuracy of the transform method increases as the number of relevant modes becomes larger, i.e., as the kernel is required only at shorter times. This will be true of the decoupling theory as well, for similar reasons. The question of the quantitative adequacy of various approximations for specific multimode systems remains to be investigated; the transform approach is likely to be inaccurate primarily (as indicated in Ref. 9) when considering strongly coupled, low frequency modes as individual scattering modes rather than as part of a heat bath.

While calculations on small model systems have a defi-

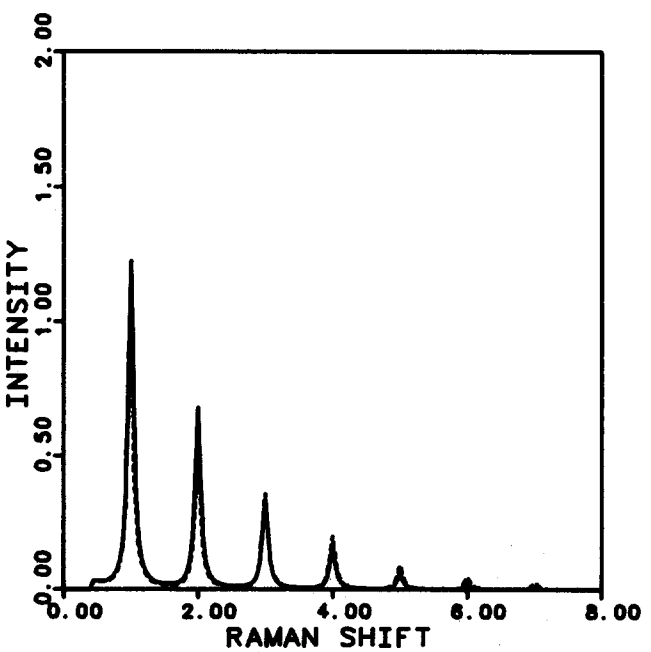

FIG. 8. Scattered profile for one mode system case 2. (—) exact; (···) decoupled approximation. $\omega_L = -1.00$, $\gamma = 0.05$, $\beta = 0.5$.

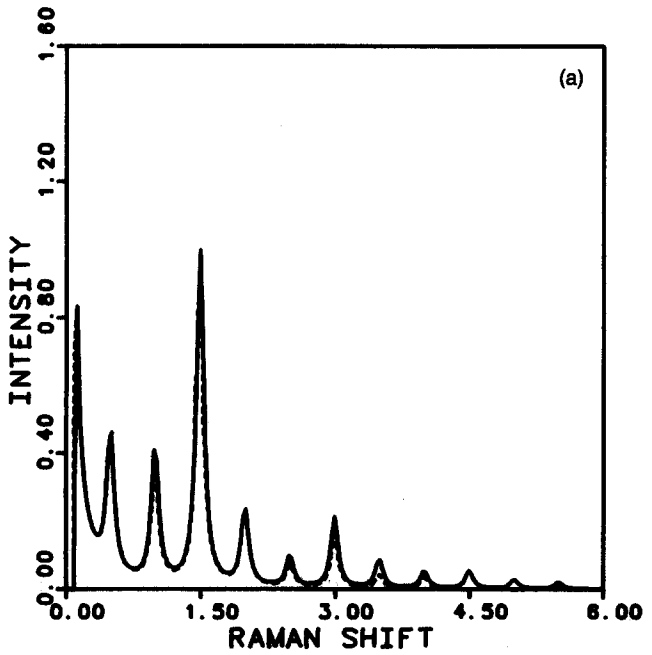

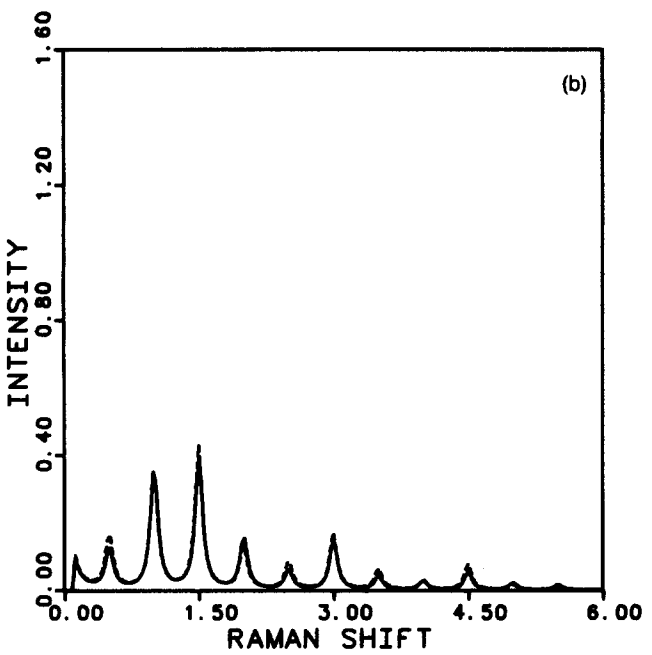

FIG. 9. Scattered profiles for two mode example. (—) exact; (···) decoupled approximation. (a) $\omega_L = -0.50$; (b) $\omega_L = +0.50$. $\gamma = 0.075$, $\beta = 0.5$.

nite heuristic value, the real utility of our method will be in modeling excitation and scattered profiles of large multidimensional systems such as transition metal complexes or protein chromophores. To simulate spectra of these systems, extensive searches of parameter space will be required before a set can be found that will simultaneously fit the wealth of experimental data available on these systems. The use of the decoupled approximation along with block factorization will facilitate this search. Once a set of parameters is found which provides a reasonable fit to the data, the calculation can be refined using the exact method. Investigations along this direction are currently in progress.

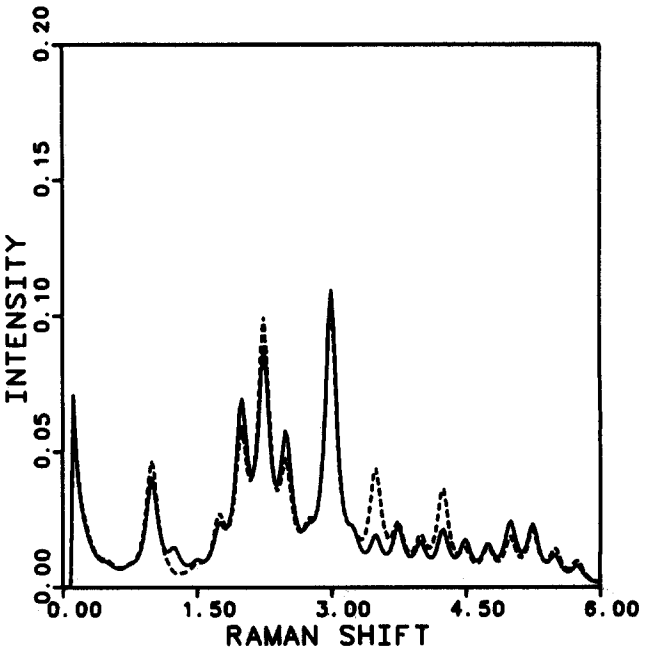

FIG. 10. Scattered profile for five mode system. (—) exact; (···) decoupled approximation. $\omega_L = 0.00$, $\gamma = 0.075$, $\beta = 1.0$.

ACKNOWLEDGMENTS

This work was supported by a grant from the National Science Foundation. RAF is an Alfred P. Sloan Foundation Fellow, 1984–1986.

APPENDIX

The Raman intensity at frequency ω can be expressed as a Fourier transform over a time-dependent kernel, $A(t,t',\mu)$:

$$i_{\alpha\gamma,\beta\lambda}(\omega) = (2\pi\hbar^2)^{-1} M_\alpha^{eg} M_\gamma^{eg} M_\beta^{ge} M_\lambda^{ge} \times \int_{-\infty}^{\infty} d\mu\, e^{i\mu\omega} \int_0^{\infty} dt \int_0^{\infty} dt' \otimes \exp[-iE(t'-t) - \Gamma(t+t')] A(t,t',\mu) ,$$

where E is the incident energy and Γ the electronic damping term. M_δ^{ge} is the matrix element of the δ component of the system's electronic transition dipole operator between the ground (g) and excited (e) states. The exact expression for the kernel within the adiabatic, Condon, and single electronic excited state approximations is (see Ref. 1)

$$K(t,t',\mu) = ZA(t,t',\mu) = \sum_n \langle n| e^{it'H^e} e^{i\mu H^g} \times e^{-itH^e} e^{-i(t'-t+\mu-i\beta)H^g} |n\rangle , \qquad \text{(A1)}$$

where Z is the partition function, and the trace is over the eigenstates of the ground state Hamiltonian H^g.

We want to show that the coefficients in the Fourier expansion of the kernel [Eq. (1)] can be factored into a form

$$F_n(t,t') = A_n(t) A_n^+(t')$$

at $T = 0$ K.

We denote eigenkets of the ground and excited state

TABLE V. Exact and approximate values for the Fourier expansion coefficients of Eq. (1) at selected values of t and t' for the two mode system in Table II. The values listed are for the fundamental of the lower frequency mode ($\omega = 1.00$) at $\beta = 1.00$.

		EXACT		APPROXIMATE					
				$\omega t_0 = 0.05$		$\omega t_0 = 0.10$		$\omega t_0 = 0.15$	
ωt	$\omega t'$	ReF(t,t')	ImF(t,t')	ReF(t,t')	ImF(t,t')	ReF(t,t')	ImF(t,t')	ReF(t,t')	ImF(t,t')
0.00	0.00	0.000	0.000	0.000	0.000	0.000	0.000	0.000	0.000
0.00	1.20	2.186×10^{-8}	-1.369×10^{-7}	2.074×10^{-8}	-1.390×10^{-7}	1.985×10^{-8}	-1.415×10^{-7}	1.919×10^{-8}	1.444×10^{-7}
0.00	2.40	-5.853×10^{-8}	-1.276×10^{-7}	-6.1511×10^{-8}	-1.285×10^{-7}	-6.460×10^{-8}	-1.299×10^{-7}	-6.782×10^{-8}	-1.319×10^{-7}
0.00	3.60	-8.189×10^{-8}	-7.679×10^{-8}	-8.404×10^{-8}	-7.633×10^{-8}	-8.650×10^{-8}	-7.623×10^{-8}	-8.919×10^{-8}	-7.647×10^{-8}
1.20	0.00	2.186×10^{-8}	1.369×10^{-7}	2.074×10^{-8}	1.390×10^{-7}	1.985×10^{-8}	1.415×10^{-7}	1.919×10^{-8}	1.444×10^{-7}
1.20	1.20	9.467×10^{-2}	-1.531×10^{-9}	9.467×10^{-2}	-4.553×10^{-9}	9.467×10^{-2}	-4.394×10^{-10}	9.467×10^{-2}	-2.941×10^{-10}
1.20	2.40	8.359×10^{-2}	-6.179×10^{-2}	8.745×10^{-2}	-5.345×10^{-2}	8.697×10^{-2}	-5.419×10^{-2}	8.642×10^{-2}	-5.499×10^{-2}
1.20	3.60	4.048×10^{-2}	-7.057×10^{-2}	4.048×10^{-2}	-7.057×10^{-2}	4.048×10^{-2}	-7.507×10^{-2}	4.048×10^{-2}	-7.057×10^{-2}
2.40	0.00	-5.853×10^{-8}	1.276×10^{-7}	-6.151×10^{-8}	1.285×10^{-7}	-6.463×10^{-8}	1.299×10^{-7}	-6.782×10^{-8}	1.319×10^{-7}
2.40	1.20	8.359×10^{-2}	6.179×10^{-2}	8.745×10^{-2}	5.345×10^{-2}	8.697×10^{-2}	5.419×10^{-2}	8.642×10^{-2}	5.499×10^{-2}
2.40	2.40	1.214×10^{-1}	-1.124×10^{-9}	1.214×10^{-1}	-1.124×10^{-9}	1.214×10^{-1}	-1.178×10^{-9}	1.214×10^{-1}	-8.870×10^{-9}
2.40	3.60	8.715×10^{-2}	-4.269×10^{-2}	8.715×10^{-2}	-4.269×10^{-2}	8.715×10^{-2}	-4.269×10^{-2}	8.715×10^{-2}	-4.269×10^{-2}
3.60	0.00	-8.189×10^{-8}	7.679×10^{-8}	-8.404×10^{-8}	7.633×10^{-8}	-8.650×10^{-8}	7.623×10^{-8}	-8.919×10^{-8}	7.647×10^{-8}
3.60	1.20	4.048×10^{-2}	7.057×10^{-2}	4.972×10^{-2}	6.439×10^{-2}	4.892×10^{-2}	6.500×10^{-2}	4.809×10^{-2}	6.562×10^{-2}
3.60	2.40	8.715×10^{-2}	4.269×10^{-2}	8.715×10^{-2}	4.269×10^{-2}	8.715×10^{-2}	4.269×10^{-2}	8.715×10^{-2}	4.269×10^{-2}
3.60	3.60	8.416×10^{-2}	-6.650×10^{-10}	8.416×10^{-2}	-9.055×10^{-10}	8.416×10^{-2}	-9.729×10^{-10}	8.416×10^{-2}	-7.572×10^{-10}

Hamiltonians by $|n\rangle$ and $|m\rangle$, respectively. By inserting a complete set of states between each pair of exponential operators, we can rewrite Eq. (A1) as

$$K(t,t',\mu) = \sum_n \sum_{n'} \sum_m \sum_{m'} \langle n|m\rangle\langle m|n'\rangle\langle n'|m'\rangle\langle m'|n\rangle \otimes e^{it'E_m} e^{-itE_{m'}} e^{-i(t'-t-i\beta)E_n} e^{i\mu(E_{n'}-E_n)} . \tag{A2}$$

At $T = 0$ only the zero phonon state is populated so the sum over n collapses to one term. The energy of this state is defined to be zero. By comparison with Eq. (1), we see that for scattering into the state $|l\rangle$,

$$F_l(t,t') = \sum_m \sum_{m'} \langle 0|m\rangle\langle m|l\rangle\langle l|m'\rangle\langle m'|0\rangle \otimes e^{itE_{m'}} e^{-it'E_m} . \tag{A3}$$

Since the sums over m and m' are independent of one another, the expression can be factorized into the form

$$F_l(t,t') = \left[\sum_{m'} \langle 0|m'\rangle\langle m'|l\rangle e^{-itE_{m'}}\right] \otimes \left[\sum_m \langle 0|m\rangle\langle m|l\rangle e^{+it'E_m}\right] . \tag{A4}$$

At finite temperature, the coefficients in Eq. (1) can be factored at short (t and t') times into a form analogous to Eq. (A4). This is most easily seen by writing the finite temperature version of Eq. (A3) as

$$F_l(t,t') = \sum_n e^{-\beta E_n} e^{-i(t'-t)E_n} \sum_m \langle n|m\rangle \times\langle m|l+n\rangle e^{-iE_{m'}t'} \sum_{m'} \langle n|m'\rangle\langle m'|l+n\rangle e^{iE_{m'}t} \tag{A5}$$

and expanding the exponentials in time to first order to give

$$F_l(t,t') = \sum_n e^{-\beta E_n}[1 - iE_n(t'-t)] \times\sum_m \langle n|m\rangle\langle m|l+n\rangle(1 - iE_m t') \otimes\sum_{m'} \langle n|m'\rangle\langle m'|l+n\rangle(1 + iE_{m'}t) . \tag{A6}$$

Defining

$$\sigma_n = \sum_m E_m\langle n|m\rangle\langle m|l+n\rangle = \sum_{m'} E_{m'}\langle n|m'\rangle\langle m'|l+n\rangle$$

and using the relation

$$\sum_m \langle n|m\rangle\langle m|l+n\rangle = \delta_{n,n+l}$$

allows Eq. (A6) to be written (for non-Rayleigh lines) as

$$F_I(t,t') = \sum_n e^{-\beta E_n} \sigma_n^2 \, tt'[1 - iE_n(t'-t)]$$
$$= tt'[\xi_1 + i(t-t')\xi_2], \qquad \text{(A7)}$$

where

$$\xi_1 = \sum_n e^{-\beta E_n} \sigma_n^2$$

and

$$\xi_2 = \sum_n E_n \, e^{-\beta E_n} \sigma_n^2 .$$

Equation (A7) can also be arrived at by writing $F_I(t,t')$ in the factorized form

$$F_I(t,t') = \xi_1^{1/2}\{t[1 + i(\xi_2/\xi_1)t]\}$$
$$\otimes \xi_1^{1/2}\{t'[1 - i(\xi_2/\xi_1)t']\},$$

which agrees with Eq. (A7) to third order and has the form $F_I(t,t') = A(t)A^{+}(t')$. Exact and approximate values of $F(t,t')$ at selected time points for $\omega = 1.00$ of the two mode system discussed in Sec. IV are shown in Table V.

[1]R. Friesner, M. Pettitt, and J. M. Jean, J. Chem. Phys. **82**, 2918 (1985).
[2]S. Y. Lee and E. J. Heller, J. Chem. Phys. **71**, 4777 (1979); D. J. Tannor and E. J. Heller, *ibid.* **77**, 202 (1982).
[3]See, for example, P. M. Champion and A. C. Albrecht, Annu. Rev. Phys. Chem. **33**, 353 (1982), and references contained therein.
[4]I. J. Tehver and V. V. Hizhnyakov, Phys. Status Solidi **21**, 755 (1967); **39**, 67 (1970); Phys. Status Solidi B **82**, K89 (1977).
[5]D. L. Tonks and J. B. Page, Chem. Phys. Lett. **66**, 449 (1979).
[6]J. B. Page and D. L. Tonks, J. Chem. Phys. **75**, 5694 (1981).
[7]D. L. Tonks and J. B. Page, Chem. Phys. Lett. **79**, 247 (1981).
[8]D. L. Tonks and J. B. Page, J. Chem. Phys. **76**, 5820 (1982).
[9]C. K. Chan and J. B. Page, J. Chem. Phys. **79**, 5234 (1983).
[10]R. Balian and E. Brezin, Nuovo Cimento B **64**, 37 (1969).
[11]R. W. Munn and R. Silbey, J. Phys. A **11**, 939 (1978).
[12]Dalquist and Bjork, *Numerical Methods* (Prentice Hall, Englewood Cliffs, NJ, 1974).
[13]C. K. Chan, J. B. Page, D. L. Tonks, O. Brafman, B. Khodadoost, and C. T. Walker, J. Chem. Phys. **82**, 4813 (1985).